

Entanglement in first excited states of some many-body quantum spin systems: indication of quantum phase transition in finite size systems

George Biswas and Anindya Biswas

*Department of Physics, National Institute of Technology Sikkim
Ravangla, South Sikkim 737139, India.*

(Dated: November 13, 2020)

We compute concurrence, a measure of bipartite entanglement, of the first excited state of the 1-D Heisenberg frustrated J_1 - J_2 spin-chain and observe a sudden change in the entanglement of the eigenstate near the coupling strength $\alpha = J_2/J_1 \approx 0.241$, where a quantum phase transition from spin-fluid phase to dimer phase has been previously reported. We numerically observe this phenomena for spin-chain with 8 sites to 16 sites, and the value of α at which the change in entanglement is observed, asymptotically tends to a value $\alpha_c \approx 0.24116$. We have calculated the finite-size scaling exponents for spin chains with even and odd spins. It may be noted that bipartite as well as multipartite entanglement measures applied on the ground state of the system, fail to detect any quantum phase transition from the gapless to the gapped phase in the 1-D Heisenberg frustrated J_1 - J_2 spin-chain. Furthermore, we measure bipartite entanglement of first excited states for other spin models like 2-D Heisenberg J_1 - J_2 model and Shastry-Sutherland model and find similar indications of quantum phase transitions.

I. INTRODUCTION

Advances in technology in the field of low temperature experiments have made it possible to engineer some quantum many-body Hamiltonians using ultracold atoms and ions [1]. Such quantum spin systems may be important as substrates for quantum computation. Quantum entanglement is a resource for quantum computational tasks. Therefore, it is important to study and understand entanglement in such systems. Bipartite and multipartite entanglement [2–7] in ground states of quantum spin systems have been studied and critical quantum phenomena [8–14] have been detected. However, entanglement of low lying excited states of quantum spin systems have not been exhaustively studied [15–17]. In this paper, we compute a nearest neighbor bipartite entanglement measure namely concurrence [18] of qubits in first excited states of some non-integrable quantum spin systems.

The systems that we have studied are the one dimensional Heisenberg frustrated $J_1 - J_2$ spin chain, the two dimensional Heisenberg $J_1 - J_2$ spin system and the Shastry-Sutherland model. The ground states of these systems have been investigated and bipartite and multipartite quantum entanglement have been measured [8]. Quantum phase transitions (QPT), a zero temperature phase transition driven by system parameters [19], have been detected in some of the cases. However, the quantum phase transition from the spin fluid phase to dimer phase has not been detected using any quantum entanglement measure for the one dimensional Heisenberg frustrated $J_1 - J_2$ spin chain. The quantum phase transition from the gapless phase to the gapped phase in the one dimensional Heisenberg frustrated $J_1 - J_2$ spin chain was investigated by Haldane [20], Tonegawa and Harada [21], Okamoto and Nomura [22] using exact diagonalization and field theory methods. It was reported that the ground state is in the gapless or gapped phase depending on the value of the coupling strength α . The

quantum phase transition point was estimated by investigating the singlet-triplet energy gap of finite size systems [21] followed by extrapolation to infinite system. In Ref. [22], the phase transition point was determined by investigating the difference between the singlet-triplet gap and the singlet-singlet gap for finite size systems. In Ref. [21, 22], the singlet-triplet energy gap was defined as

$$G_{st}(N, \alpha) \equiv E_1^{(0)}(N, \alpha) - E_0^{(0)}(N, \alpha) \quad (1)$$

while the singlet-singlet energy gap was defined as

$$G_{ss}(N, \alpha) \equiv E_0^{(1)}(N, \alpha) - E_0^{(0)}(N, \alpha) \quad (2)$$

where $E_m^{(0)}(N, \alpha)$ and $E_m^{(l)}(N, \alpha)$ are the ground state energy and the l th excited state energy in the $S_{total} = m$ subspace, respectively. The first excited states of the systems, considered in this paper, are in general, degenerate. Let $|E_1^i\rangle$ denote the i -th degenerate eigenstate corresponding to the eigenenergy E_1 . Then the density matrix corresponding to the first excited d -fold degenerate eigenstate is given by

$$\rho_1 = \frac{1}{d} \sum_{i=1}^d |E_1^i\rangle \langle E_1^i| \quad (3)$$

Note that in this paper we do not consider different total spin subspaces explicitly.

We measure the nearest neighbor concurrence of the first excited state ρ_1 of the spin chain, and notice a sudden change in the value of concurrence near the quantum phase transition point [22, 23]. The computation along-with the appropriate scaling analysis is done for spin chains consisting of 8 to 16 qubits. The scaling analysis and the corresponding finite size scaling exponents are different for even and odd spin chains. The quantum critical point $\alpha_c \approx 0.24116$ is estimated from the scaling analysis of spin chains with even number of qubits.

The finite size scaling exponent $\beta = -1.962$. The concurrence versus driving parameter plot Fig. 1 for spin chains with odd number of qubits shows two discontinuities with both of them converging to the quantum phase transition point in the asymptotic limit. The scaling exponent of the right shifting and left shifting discontinuities are $\beta_R = -1.92$ and $\beta_L = -2.082$ respectively. The nearest neighbor concurrence of first excited states of the two dimensional Heisenberg $J_1 - J_2$ spin system and the Shastry-Sutherland model for 16 qubits in a (4×4) sites square lattice have also been calculated. We get indications of quantum phase transition in both the systems.

In Section II, we discuss the results for the one dimensional Heisenberg $J_1 - J_2$ model in details and highlight the importance of investigating the low lying excited states in quantum spin systems. In Sections III and IV we discuss the results obtained for the two dimensional Heisenberg's $J_1 - J_2$ model and Shastry-Sutherland spin model respectively. Finally, we conclude in Section V.

II. THE ONE DIMENSIONAL HEISENBERG $J_1 - J_2$ SPIN CHAIN

We consider the Heisenberg frustrated one dimensional $J_1 - J_2$ model in which the nearest neighbor couplings J_1 and the next nearest neighbor couplings J_2 are both antiferromagnetic. The Hamiltonian of the system is given by

$$H_{1D} = J_1 \sum_{i=1}^N \vec{\sigma}_i \cdot \vec{\sigma}_{i+1} + J_2 \sum_{i=1}^N \vec{\sigma}_i \cdot \vec{\sigma}_{i+2} \quad (4)$$

Here, N represents the number of sites present in the spin chain, J_1 and J_2 are antiferromagnetic coupling coefficients of nearest and next nearest neighbor interactions and $\vec{\sigma} = \sigma^x \hat{x} + \sigma^y \hat{y} + \sigma^z \hat{z}$ where $\sigma^x, \sigma^y, \sigma^z$ are the Pauli spin matrices. Some solid state systems like $SrCuO_2$ may be described by this Hamiltonian [24]. Periodic boundary condition, $\sigma_{N+1} = \sigma_1$, has been imposed on all systems that have been investigated in this paper. It was known previously that this spin system goes from spin-fluid phase to dimer phase around $\alpha = J_2/J_1 \approx 0.241$. In the weakly frustrated region, $0 < \alpha < 0.24$ the system is gapless while it enters a gapped region for higher values of the coupling parameter [25–27].

It may be noted that for a two qubit state ρ , concurrence C is defined as [18] $\max(0, \lambda_1 - \lambda_2 - \lambda_3 - \lambda_4)$, where λ_i 's are the square roots of eigenvalues of $\rho(\sigma^y \otimes \sigma^y)\rho^*(\sigma^y \otimes \sigma^y)$ in decreasing order and ρ^* is complex conjugate of ρ . We perform exact diagonalization of the system Hamiltonian for system sizes $N = 8$ to $N = 15$. For large spin chains ($N > 15$) we are unable to use the exact diagonalization technique to calculate the eigenvalues and eigenvectors due to memory constraint of the computers used for computation. For $N = 16$, we use ARPACK (available in MATLAB that uses lanczos algorithm) to calculate first 6 low lying eigen states. The

results obtained using the Lanczos algorithm is compared with exact diagonalization results for system sizes up to $N = 15$ and both the eigenvalues and eigenvectors are found to be fairly accurate. We find the ground state and the low lying excited states and calculate the nearest neighbor concurrence, after tracing out the other qubits. In Fig. 1 (a), we plot the nearest neighbor concurrence for the first excited states for the systems with even number of qubits from $N = 8$ to $N = 16$ and notice discontinuities in the plots in the vicinity of the quantum phase transition point. In Fig. 1 (b), we plot the nearest neighbor concurrence for the first excited states for the systems with odd number of qubits from $N = 9$ to $N = 15$ and notice a pair of discontinuities in the plots in the vicinity of the quantum phase transition point. Finite size scaling analysis is done for data obtained for both even and odd spin chains to ascertain the behavior of the systems as $N \rightarrow \infty$. In Fig. 2, we plot the nearest neighbor concurrence of the ground state as well as of the first excited state for the spin chain with $N = 16$. The plot of nearest neighbor concurrence for qubits is continuous across the QPT point for the ground state of the system whereas we notice a sudden drop in the value of concurrence in the vicinity of the quantum critical point at $\alpha_c^{16} = 0.24248$. The discontinuity of the bipartite entanglement of the first excited state of the system indicates the quantum phase transition point whereas a similar probe applied to the ground state of the same system fails to indicate the quantum phase transition.

$N_{(even)}$	$\alpha_c^{N_{(even)}}$	$N_{(odd)}$	$\alpha_{c,R}^{N_{(odd)}}$	$\alpha_{c,L}^{N_{(odd)}}$
8	0.24630	9	0.10855	0.33049
10	0.24449	11	0.14910	0.29944
12	0.24349	13	0.17465	0.28243
14	0.25288	15	0.19145	0.27199
16	0.24248			

TABLE I. The driving parameter corresponding to the discontinuities in the nearest neighbor concurrence is listed against the appropriate number of qubits.

In Table I, we have listed the values of the driving parameters at the discontinuities of the nearest neighbor concurrence of the first excited states for spin chains of $N = 8$ to $N = 16$ qubits. Similar results for even number of qubits were found earlier using conformal field theory by K. Okamoto and K. Nomura [22] for the QPT point, and our calculated values match with their results up to the fourth decimal place. The discontinuities associated with even spin chains are closer to the quantum phase transition point. The numerical values of α_c^N decrease with increasing N , for even number of qubits and asymptotically tend towards a fixed value α_c . We fit a rational function $F(N)$ with second degree polynomials in numerator and denominator through the tabulated values

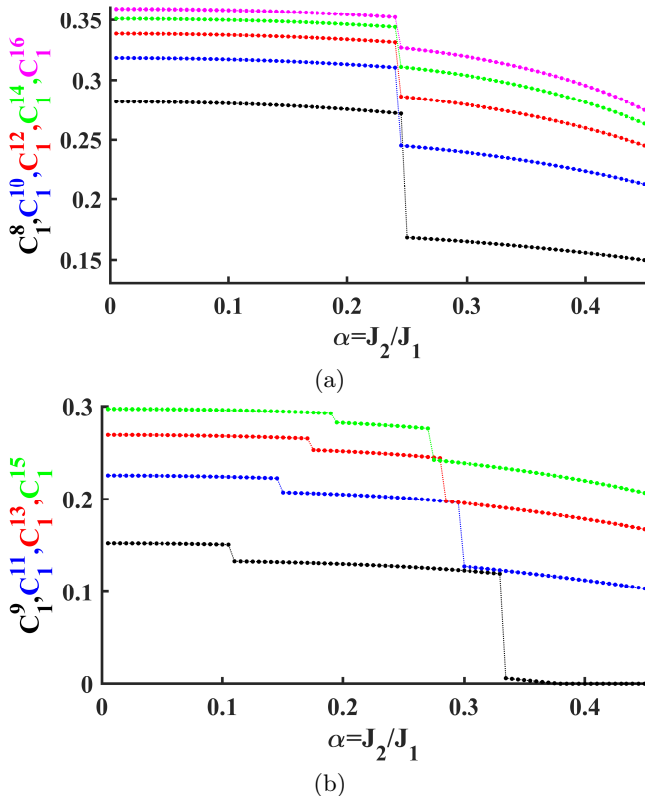


FIG. 1. (color online) Nearest neighbor concurrence in ebits of the first excited state of the 1-D $J_1 - J_2$ Hamiltonian is plotted with respect to the dimensionless system parameter α , (a) for spin chains with even number of qubits and (b) for spin chains with odd number of qubits.

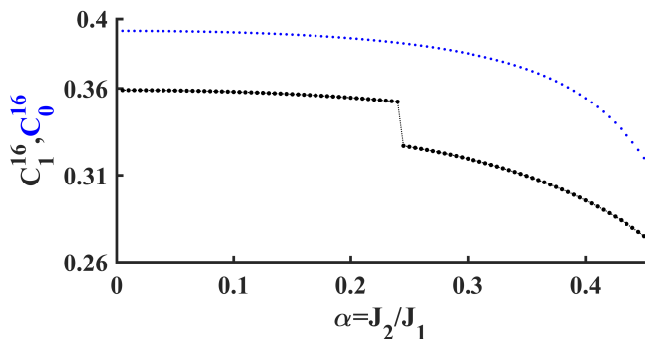


FIG. 2. (color online) Nearest neighbor concurrence in ebits of the ground state and first excited state of 1-D $J_1 - J_2$ Hamiltonian is plotted with respect to dimensionless system parameter α for system size $N = 16$ (using partial ARPACK diagonalization). The solid black dots represent first excited state concurrence (C_1^{16}) and smaller blue dots represent ground state concurrence (C_0^{16}).

associated with even spin chains;

$$F(N) = \frac{p_1 N^2 + p_2 N + p_3}{N^2 + q_1 N + q_2} \quad (5)$$

where $p_1 = 0.2412$, $p_2 = 0.1477$, $p_3 = 0.4848$, $q_1 =$

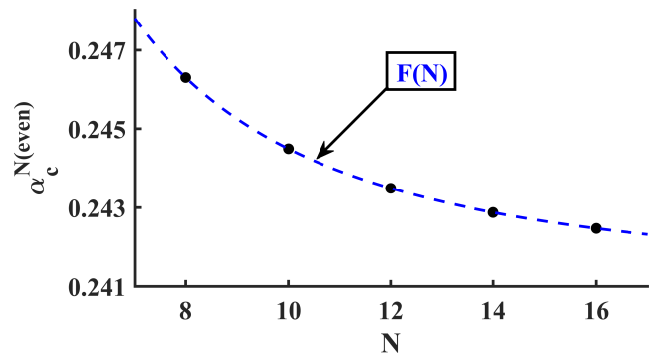


FIG. 3. (color online) The position of discontinuities of the nearest neighbor concurrence $\alpha_c^{N(even)}$ is plotted with respect to system size N . $F(N)$ is the curve fitted through these points.

0.6151, and $q_2 = 0.5081$. In Fig. 3 we plot the position of discontinuities of the nearest neighbor concurrence $\alpha_c^{N(even)}$ with respect to system size N . We choose the rational function because of its known advantages in extrapolation. The QPT point is estimated to be at $\alpha_c \approx 0.24116$ from the extrapolated function.

It may be noted that there are two discontinuities in nearest neighbor concurrence of odd spin chains which appear to asymptotically converge to some point of the system parameter α . We have listed the right shifting as well as left shifting discontinuities for spin chains with odd number of particles from $N = 9$ to $N = 15$ in Table. I. To study the convergence of the two discontinuities and to gain further insight into finite size quantum spin systems engineered in the laboratories, we study the scaling of the QPT points with respect to N .

In Fig. 4 (a) we plot $\log_2(\alpha_c^{N(even)} - \alpha_c)$ with respect to $\log_2(N)$. We find that a straight line fits the plot, the equation of which is obtained by the method of least squares. The sum of squares due to errors (SSE), which measures the total deviation of the fit from the response values, associated with the straight line fit is 5.5561×10^{-5} . The equation of the straight line is given by

$$\log_2(\alpha_c^{N(even)} - \alpha_c) = \beta \log_2(N) + c \quad (6)$$

with, $\beta = -1.962$ and $c = -1.715$. We may write equation 6 as

$$\alpha_c^{N(even)} = \alpha_c + 0.3046 N^{-1.962} \quad (7)$$

From the previous equation we note that $\alpha_c^{N(even)}$ approaches α_c as $N^{-1.962}$. The scaling exponent obtained, using this method of detection of QPT point, $\beta = -1.962$ is significantly high. We use the value of α_c obtained by analysing the even spin chains for the scaling analysis of odd spin chains. In Fig. 4 (b) and Fig. 4 (c) we plot $\log_2(\alpha_{c,R}^{N(odd)} - \alpha_c)$ and $\log_2(\alpha_{c,L}^{N(odd)} - \alpha_c)$ with respect to $\log_2(N)$, to study the right-shifting and left-shifting

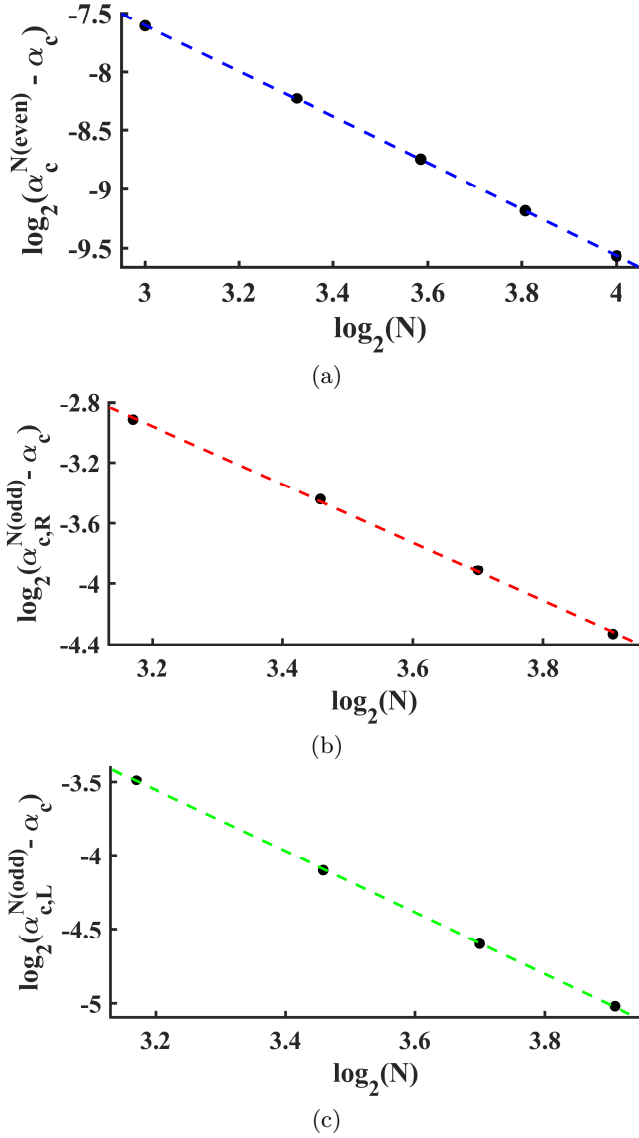


FIG. 4. (color online) (a) $\log_2(\alpha_c^{N^{(even)}} - \alpha_c)$ versus $\log_2(N)$ plot, (b) $\log_2(\alpha_c^{N^{(odd)}} - \alpha_c)$ versus $\log_2(N)$ plot and (c) $\log_2(\alpha_c^{N^{(odd)}} - \alpha_c)$ versus $\log_2(N)$ plot.

discontinuities of odd spin chains. The SSE associated with the plots are 7.2094×10^{-4} and 1.3726×10^{-4} respectively and the corresponding equations may be written as

$$\alpha_{c,R}^{N^{(odd)}} = \alpha_c + 9.082 N^{-1.92} \quad (8)$$

$$\alpha_{c,L}^{N^{(odd)}} = \alpha_c + 8.64 N^{-2.082}. \quad (9)$$

The data points for the odd spin chains fit very well in the finite size scaling plot and the right and left shifting discontinuities approach α_c as $N^{-1.92}$ and $N^{-2.082}$ respectively.

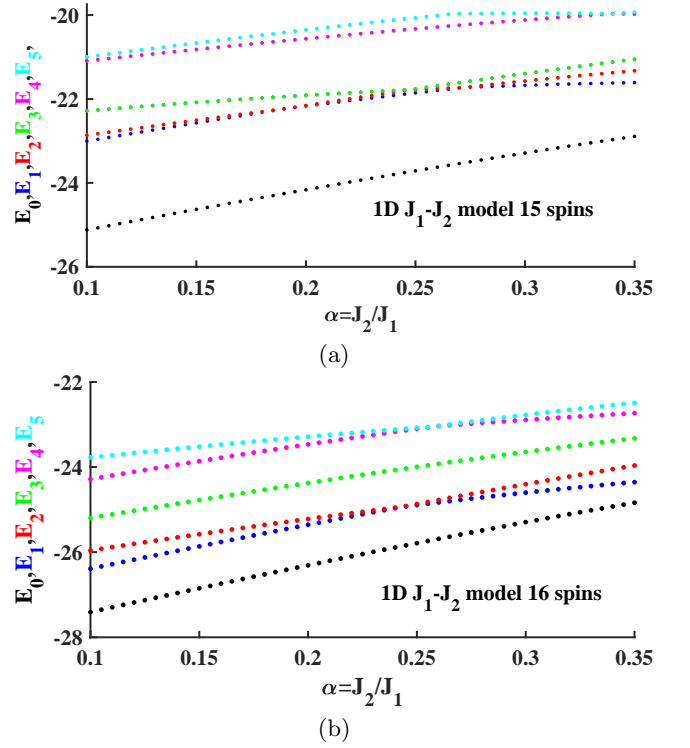


FIG. 5. (color online) Energy levels of ground and low lying excited states are plotted with respect to the dimensionless driving parameter α of the (a) frustrated $J_1 - J_2$ spin chain with odd number of qubits, (b) frustrated $J_1 - J_2$ spin chain with even number of qubits.

It may be noted that a previous investigation of the same spin chain for even number of qubits by Chen *et al.* [28] focused on the fidelity of adjacent pure ground states and excited states as a function of the driving parameter α . It was reported that the adjacent ground state fidelity practically remains constant and equal to 1 for $0 < \alpha < 0.5$. However, the fidelity of adjacent first excited states deviates from 1 close to the quantum phase transition point. From the energy level diagram Fig. 5 (b) it can be seen that there is no level crossing for ground state for finite size systems in the parameter range $0 \leq \alpha \leq 0.35$. Note that the first and second excited energy levels cross in the vicinity of the quantum phase transition point. In a paper by G.S.Tian and H.Q.Lin [29], it was shown that level crossing of low lying excited states causes quantum phase transition when there is no ground state level crossing. For the case of spin chains with odd number of qubits we find two discontinuities and observe that both the discontinuities approach towards the same quantum phase transition point. We may clearly see the reason of the two discontinuities from the energy level diagram Fig. 5 (a) of 15 qubits spin chain – there are actually two level crossings between the first and second excited states. In Ref. [21], the authors had considered the singlet-triplet energy gap as an indicator of quantum phase transition. The phase transition point was determined (≈ 0.3) by

extrapolating the singlet-triplet energy gap for infinite spin chain. The singlet state with energy $E_0^0(N, \alpha)$ is the ground state of the system while the triplet state with energy $E_1^0(N, \alpha)$ is the first excited state of the spin chain before the quantum phase transition point. The triplet state with energy $E_1^0(N, \alpha)$ becomes the second excited state for $\alpha > \alpha_c$. In Ref. [22] the authors considered the difference between the singlet-singlet energy gap and the singlet-triplet energy gap as an indicator of quantum phase transition. The analysis was done for finite size spin chains. The singlet-singlet energy gap defined in Eq. 2, is the difference of energy of the ground and second excited states of the spin system before the quantum phase transition point while it is the difference between the ground and first excited states after the phase transition point. The phase transition point was determined at $\alpha_c = 0.2411$ by extrapolation. The method for detection of quantum phase transition, using the entanglement of first excited state as an indicator, relies on the crossing of the first and second excited states for finite size spin chains. The difference between the singlet-singlet energy gap and the singlet-triplet energy gap becomes zero [22] at the point of intersection of the first and second excited energy levels. The fidelity of the first excited pure state dips at the point of phase transition also due to the intersection of the first and second excited energy levels.

III. THE TWO DIMENSIONAL HEISENBERG $J_1 - J_2$ SPIN SYSTEM

We consider an arrangement of qubits in two dimensional square lattice, where the nearest neighbor spins are coupled by Heisenberg interactions, with coupling strength J_1 and the next nearest neighbor or diagonal spins are coupled by the same interactions with coupling strength J_2 . The coupling strengths J_1 and J_2 are positive. Magnetic materials such as $Li_2VO SiO_4$ and $Li_2VO GeO_4$ can be described by this Hamiltonian [30–34]. We measure first excited state nearest neighbor concurrence in a square lattice with (4×4) sites. The system Hamiltonian is given by

$$H_{2D} = J_1 \sum \vec{\sigma}_i \cdot \vec{\sigma}_j + J_2 \sum \vec{\sigma}_i \cdot \vec{\sigma}_k \quad (10)$$

where i, j are nearest neighbors (horizontal or vertical) and i, k are next nearest neighbors or diagonal spins. J_1 and J_2 are antiferromagnetic. Periodic boundary condition is imposed during computation. The spin model has been studied using exact diagonalization, field theory methods [35–37], but the exact phase boundaries are not known. It is predicted that there are two long range ordered phases separated by quantum paramagnetic phase without long range order, in the system. It has also been predicted that quantum phase transitions exist from ‘ordinary-*Néel* order’ to intermediate phase and from that intermediate phase to ‘colinear-*Néel* order’ at $\alpha \approx 0.4$ and $\alpha \approx 0.6$ respectively [38, 39]. The inter-

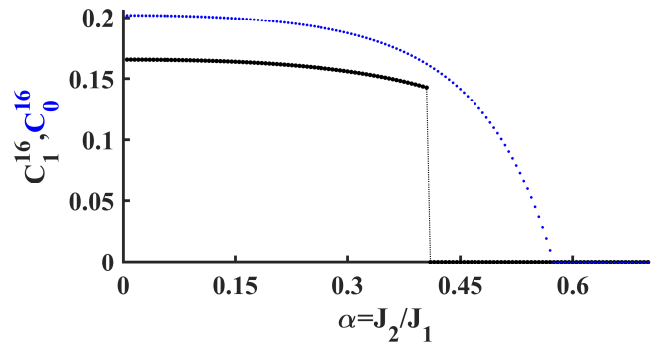


FIG. 6. (color online) Nearest neighbor concurrence in ebits of the ground state and first excited state of the 2-D $J_1 - J_2$ Hamiltonian is plotted with respect to dimensionless system parameter α for system size $N = 16$ (using partial ARPACK diagonalization). The solid black dots represent first excited state concurrence (C_1^{16}) and smaller blue dots represent ground state concurrence (C_0^{16}).

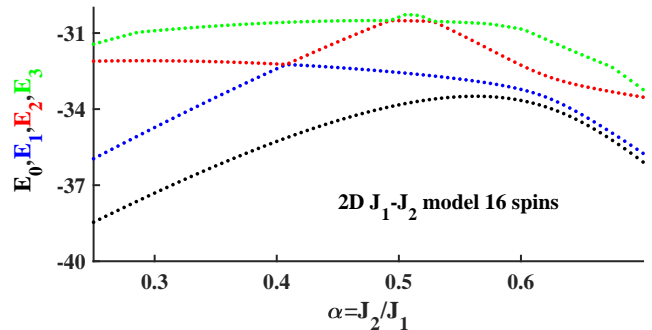


FIG. 7. (color online) Energy levels of ground and low lying excited states are plotted with respect to the dimensionless driving parameter α of the 2-dimensional frustrated $J_1 - J_2$ spin system with 16 (4×4) qubits.

mediate phase [40] is predicted as plaquette or columnar dimer phase [41–49] as well as spin fluid phase [50–52].

It can be seen from Fig. 6 that the nearest neighbor concurrence of the ground state goes to zero and indicates the intermediate to collinear-*Néel* phase QPT at $\alpha = 0.58$. Further, there is a sudden disappearance of nearest neighbor concurrence of the first excited state at $\alpha = 0.4078$, indicating the ordinary-*Néel* to intermediate phase QPT point. Note that the ground state nearest neighbor concurrence does not detect the ordinary-*Néel* to intermediate phase QPT point. Similar to the one dimensional case here also we see from the energy level diagram, Fig. 7, that there is a level crossing between the first and second excited states in the vicinity of the quantum phase transition point.

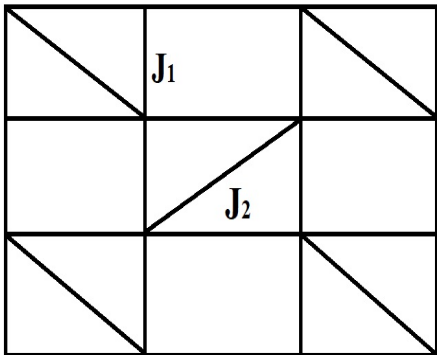


FIG. 8. The Shastry-Sutherland lattice with 16 sites. The horizontal and vertical lines represent nearest neighbor coupling strength J_1 and the specific diagonal lines represent next nearest neighbor coupling strength J_2 .

IV. THE SHASTRY-SUTHERLAND SPIN SYSTEM

We study the entanglement properties of the first excited state of the Shastry-Sutherland quantum spin Hamiltonian for a (4×4) square lattice, the schematic diagram of which is shown in Fig. 8.

The Hamiltonian of the spin system is given by

$$H_{SS} = J_1 \sum \vec{\sigma}_i \cdot \vec{\sigma}_j + J_2 \sum \vec{\sigma}_k \cdot \vec{\sigma}_l \quad (11)$$

where i, j are the nearest neighbors (horizontal and vertical) and k, l are the specific diagonal pairs [53] shown in Fig. 8. The coupling strengths J_1 and J_2 are both positive. Periodic boundary condition is imposed during computation.

It is predicted that the system goes through two quantum phase transitions from *Néel* to intermediate phase and from intermediate phase to dimer, driven by quantum fluctuations [54, 55]. The nature of the intermediate phase is not yet known. The quantum phase transition from an intermediate phase to dimer phase has been predicted by bipartite as well as multipartite entanglement measures applied on the ground state of the system [8] at $\alpha \approx 1.53$. However, for this system a multipartite entanglement measure, namely the generalised geometric measure applied on the ground state of the system detects both the quantum critical points, from *Néel* to intermediate phase at $\alpha \approx 1.05$ and from intermediate phase to dimer at $\alpha \approx 1.53$.

In Fig. 9, we note that for $\alpha \geq 1.52798$ the nearest neighbor concurrence of the first excited eigenstate of the Hamiltonian H_{SS} (C_1^{16}) suddenly becomes zero. The drop in the value of concurrence is sudden indicating the quantum phase transition. Similar to the other models, we see from Fig. 10 that there is a level crossing between first and second excited energy levels in the vicinity of quantum phase transition point.

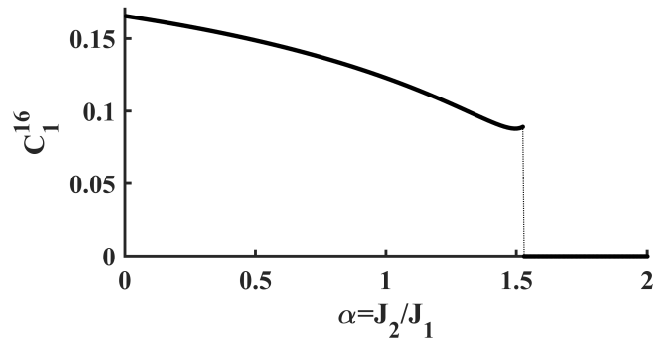


FIG. 9. (color online) Nearest neighbor concurrence in ebits of the first excited state of the Shastry-Sutherland Hamiltonian (C_1^{16}) is plotted with respect to the dimensionless driving parameter α for system size $N = 16$ (using partial ARPACK diagonalization).

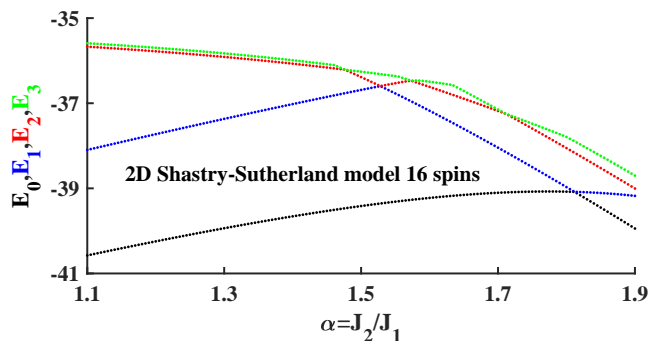


FIG. 10. (color online) Energy levels of ground and low lying excited states are plotted with respect to the dimensionless driving parameter α of the Shastry-Sutherland spin model with 16 (4×4) qubits.

V. CONCLUSIONS

We have investigated the 1D Heisenberg $J_1 - J_2$ spin chain, the 2D Heisenberg $J_1 - J_2$ spin system and the Shastry-Sutherland spin system from the viewpoint of bipartite entanglement of their low-lying eigen states. The quantum phase transition points and the phase diagrams of the above mentioned many-body spin systems have often been studied in the past [8, 22, 23, 40, 54–57]. However, there remains a few unanswered questions regarding the behavior of such systems with respect to their quantum phase diagrams. We find that the bipartite quantum entanglement measure, concurrence of nearest neighbors in first excited states, is discontinuous with the variation of the driving parameter across the quantum phase transition points. It is pertinent to mention that no physical system may be cooled to absolute zero and the low lying excited states of the system are likely to influence the behavior of the system near absolute zero temperature. Furthermore, entanglement entropy has been measured in quantum many-body systems [58] and detection of various quantum entangle-

ment measures have also been reported [59], making the present study viable for experimental investigation.

It may be noted that bipartite and multipartite quantum entanglement measures applied on the ground state of the system Hamiltonian [8] are unable to detect the quantum phase transition point for the 1D Heisenberg $J_1 - J_2$ spin system. The finite size scaling exponents, obtained using the present investigation for the 1D Heisenberg $J_1 - J_2$ model, are also quite high. The investigation of low-lying excited states of such many-body Hamiltonians promises to shed more light on the behavior of quantum spin sys-

tems.

ACKNOWLEDGMENTS

We sincerely acknowledge the “PARAM-Kanchenjunga High Performance Computer Centre, National Institute of Technology Sikkim” for the support to conduct this research. We thank Ujjwal Sen for critical comments.

-
- [1] C. S. Chiu, G. Ji, A. Mazurenko, D. Greif, and M. Greiner, Quantum state engineering of a Hubbard system with ultracold fermions, *Phys. Rev. Lett.* **120**, 243201 (2018).
- [2] R. Horodecki, P. Horodecki, M. Horodecki, and K. Horodecki, Quantum entanglement, *Rev. Mod. Phys.* **81**, 865 (2009).
- [3] A. Sen(De) and U. Sen, Channel capacities versus entanglement measures in multipartite quantum states, *Phys. Rev. A* **81**, 012308 (2010).
- [4] B. Jungnitsch, T. Moroder, and O. Gühne, Taming multipartite entanglement, *Phys. Rev. Lett.* **106**, 190502 (2011).
- [5] K. Schwaiger and B. Kraus, Relations between bipartite entanglement measures, *Quantum Information and Computation* **18**, 85 (2017).
- [6] G. Vidal and R. F. Werner, Computable measure of entanglement, *Phys. Rev. A* **65**, 032314 (2002).
- [7] L. Amico, R. Fazio, A. Osterloh, and V. Vedral, Entanglement in many-body systems, *Rev. Mod. Phys.* **80**, 517 (2008).
- [8] A. Biswas, R. Prabhu, A. Sen(De), and U. Sen, Genuine-multipartite-entanglement trends in gapless-to-gapped transitions of quantum spin systems, *Phys. Rev. A* **90**, 032301 (2014).
- [9] J. Eisert, M. Cramer, and M. B. Plenio, Colloquium: Area laws for the entanglement entropy, *Rev. Mod. Phys.* **82**, 277 (2010).
- [10] P. Calabrese and J. Cardy, Entanglement entropy and conformal field theory, *J. Phys. A Math. Theor.* **42**, 504005 (2009).
- [11] J. I. Latorre, E. Rico, and G. Vidal, Ground state entanglement in quantum spin chains, *Quantum Info. Comput.* **4**, 48 (2004).
- [12] C. Dunning, J. Links, and H.-Q. Zhou, Ground-state entanglement of the BCS model, *Phys. Rev. Lett.* **94**, 227002 (2005).
- [13] T. J. Osborne and M. A. Nielsen, Entanglement in a simple quantum phase transition, *Phys. Rev. A* **66**, 032110 (2002).
- [14] J. I. Latorre and A. Riera, A short review on entanglement in quantum spin systems, *J. Phys. A Math. Theor.* **42**, 504002 (2009).
- [15] M. Reuquardt, Entanglement-entropy for ground-states, low-lying and highly excited eigenstates of general (lattice) Hamiltonians, arXiv preprint hep-th/0605142 (2006).
- [16] V. Alba, M. Fagotti, and P. Calabrese, Entanglement entropy of excited states, *J. Stat. Mech.* **2009**, P10020 (2009).
- [17] L. Masanes, Area law for the entropy of low-energy states, *Phys. Rev. A* **80**, 052104 (2009).
- [18] S. Hill and W. K. Wootters, Entanglement of a pair of quantum bits, *Phys. Rev. Lett.* **78**, 5022 (1997).
- [19] S. Sachdev, *Quantum Phase Transitions*, 2nd ed. (Cambridge University Press, 2011).
- [20] F. D. M. Haldane, Spontaneous dimerization in the $s = \frac{1}{2}$ Heisenberg antiferromagnetic chain with competing interactions, *Phys. Rev. B* **25**, 4925 (1982).
- [21] T. Tonegawa and I. Harada, Ground-state properties of the one-dimensional isotropic spin-1/2 Heisenberg antiferromagnet with competing interactions, *Journal of the Physical Society of Japan* **56**, 2153 (1987), <https://doi.org/10.1143/JPSJ.56.2153>.
- [22] K. Okamoto and K. Nomura, Fluid-dimer critical point in $s = 12$ antiferromagnetic Heisenberg chain with next nearest neighbor interactions, *Physics Letters A* **169**, 433 (1992).
- [23] S. Eggert, Numerical evidence for multiplicative logarithmic corrections from marginal operators, *Phys. Rev. B* **54**, R9612 (1996).
- [24] M. Matsuda and K. Katsumata, Magnetic properties of a quasi-one-dimensional magnet with competing interactions: SrCuO₂, *J. Magn. Magn. Mater.* **140-144**, 1671 (1995), international Conference on Magnetism.
- [25] C. K. Majumdar and D. K. Ghosh, On next-nearest-neighbor interaction in linear chain. ii, *Journal of Mathematical Physics* **10**, 1399 (1969).
- [26] S.-J. Gu, H. Li, Y.-Q. Li, and H.-Q. Lin, Entanglement of the Heisenberg chain with the next-nearest-neighbor interaction, *Phys. Rev. A* **70**, 052302 (2004).
- [27] S. R. White and I. Affleck, Dimerization and incommensurate spiral spin correlations in the zigzag spin chain: Analogies to the Kondo lattice, *Phys. Rev. B* **54**, 9862 (1996).
- [28] S. Chen, L. Wang, S.-J. Gu, and Y. Wang, Fidelity and quantum phase transition for the Heisenberg chain with next-nearest-neighbor interaction, *Phys. Rev. E* **76**, 061108 (2007).
- [29] G.-S. Tian and H.-Q. Lin, Excited-state level crossing and quantum phase transition in one-dimensional correlated fermion models, *Phys. Rev. B* **67**, 245105 (2003).

- [30] R. Melzi, P. Carretta, A. Lascialfari, M. Mambrini, M. Troyer, P. Millet, and F. Mila, $\text{Li}_2\text{VO}(\text{si}, \text{ge})\text{O}_4$, a prototype of a two-dimensional frustrated quantum heisenberg antiferromagnet, *Phys. Rev. Lett.* **85**, 1318 (2000).
- [31] H. Rosner, R. R. P. Singh, W. H. Zheng, J. Oitmaa, S.-L. Drechsler, and W. E. Pickett, Realization of a large j_2 quasi-2d spin-half heisenberg system: $\text{Li}_2\text{VOSiO}_4$, *Phys. Rev. Lett.* **88**, 186405 (2002).
- [32] R. Nath, A. A. Tsirlin, H. Rosner, and C. Geibel, Magnetic properties of $\text{BaCdVO}(\text{PO}_4)_2$: A strongly frustrated spin- $\frac{1}{2}$ square lattice close to the quantum critical regime, *Phys. Rev. B* **78**, 064422 (2008).
- [33] T. Yildirim, Origin of the 150-k anomaly in *lafeaso*: Competing antiferromagnetic interactions, frustration, and a structural phase transition, *Phys. Rev. Lett.* **101**, 057010 (2008).
- [34] Q. Si and E. Abrahams, Strong correlations and magnetic frustration in the high T_c iron pnictides, *Phys. Rev. Lett.* **101**, 076401 (2008).
- [35] J. Richter and J. Schulenburg, The spin-1/2 j_1 - j_2 heisenberg antiferromagnet on the square lattice: Exact diagonalization for $n=40$ spins, *The European Physical Journal B* **73**, 117 (2010).
- [36] J.-K. Kim and M. Troyer, Low temperature behavior and crossovers of the square lattice quantum heisenberg antiferromagnet, *Phys. Rev. Lett.* **80**, 2705 (1998).
- [37] T. Pardini and R. R. P. Singh, Spin correlations near the edge as probe of dimer order in square-lattice heisenberg models, *Phys. Rev. B* **79**, 094413 (2009).
- [38] H. J. Schulz and T. A. L. Ziman, Finite-size scaling for the two-dimensional frustrated quantum heisenberg antiferromagnet, *Europhysics Letters (EPL)* **18**, 355 (1992).
- [39] T. Einarsson and H. J. Schulz, Direct calculation of the spin stiffness in the j_1 - j_2 heisenberg antiferromagnet, *Phys. Rev. B* **51**, 6151 (1995).
- [40] A. Metavitsiadis, D. Sellmann, and S. Eggert, Spin-liquid versus dimer phases in an anisotropic J_1 - J_2 frustrated square antiferromagnet, *Phys. Rev. B* **89**, 241104 (2014).
- [41] M. P. Gelfand, Series investigations of magnetically disordered ground states in two-dimensional frustrated quantum antiferromagnets, *Phys. Rev. B* **42**, 8206 (1990).
- [42] O. A. Starykh and L. Balents, Dimerized phase and transitions in a spatially anisotropic square lattice antiferromagnet, *Phys. Rev. Lett.* **93**, 127202 (2004).
- [43] J. Reuther and P. Wölfle, J_1 - J_2 frustrated two-dimensional heisenberg model: Random phase approximation and functional renormalization group, *Phys. Rev. B* **81**, 144410 (2010).
- [44] L. Isaev, G. Ortiz, and J. Dukelsky, Hierarchical mean-field approach to the J_1 - J_2 heisenberg model on a square lattice, *Phys. Rev. B* **79**, 024409 (2009).
- [45] A. V. Chubukov and T. Jolicoeur, Dimer stability region in a frustrated quantum heisenberg antiferromagnet, *Phys. Rev. B* **44**, 12050 (1991).
- [46] M. Mambrini, A. Läuchli, D. Poilblanc, and F. Mila, Plaquette valence-bond crystal in the frustrated heisenberg quantum antiferromagnet on the square lattice, *Phys. Rev. B* **74**, 144422 (2006).
- [47] J. Sirker, Z. Weihong, O. P. Sushkov, and J. Oitmaa, j_1 - j_2 model: First-order phase transition versus deconfinement of spinons, *Phys. Rev. B* **73**, 184420 (2006).
- [48] K. Takano, Y. Kito, Y. Ōno, and K. Sano, Nonlinear σ model method for the J_1 - J_2 heisenberg model: Disordered ground state with plaquette symmetry, *Phys. Rev. Lett.* **91**, 197202 (2003).
- [49] R. Darradi, O. Derzhko, R. Zinke, J. Schulenburg, S. E. Krüger, and J. Richter, Ground state phases of the spin-1/2 J_1 - J_2 heisenberg antiferromagnet on the square lattice: A high-order coupled cluster treatment, *Phys. Rev. B* **78**, 214415 (2008).
- [50] H.-C. Jiang, H. Yao, and L. Balents, Spin liquid ground state of the spin- $\frac{1}{2}$ square J_1 - J_2 heisenberg model, *Phys. Rev. B* **86**, 024424 (2012).
- [51] W.-J. Hu, F. Becca, A. Parola, and S. Sorella, Direct evidence for a gapless Z_2 spin liquid by frustrating néel antiferromagnetism, *Phys. Rev. B* **88**, 060402 (2013).
- [52] T. Li, F. Becca, W. Hu, and S. Sorella, Gapped spin-liquid phase in the J_1 - J_2 heisenberg model by a bosonic resonating valence-bond ansatz, *Phys. Rev. B* **86**, 075111 (2012).
- [53] B. S. Shastry and B. Sutherland, Exact ground state of a quantum mechanical antiferromagnet, *Physica B+C* **108**, 1069 (1981).
- [54] C. H. Chung, J. B. Marston, and S. Sachdev, Quantum phases of the shastry-sutherland antiferromagnet: Application to $\text{SrCu}_2(\text{BO}_3)_2$, *Phys. Rev. B* **64**, 134407 (2001).
- [55] M. Albrecht and F. Mila, First-order transition between magnetic order and valence bond order in a 2d frustrated heisenberg model, *Europhysics Letters (EPL)* **34**, 145 (1996).
- [56] W. Zheng, J. Oitmaa, and C. J. Hamer, Phase diagram of the shastry-sutherland antiferromagnet, *Phys. Rev. B* **65**, 014408 (2001).
- [57] A. Koga and N. Kawakami, Quantum phase transitions in the shastry-sutherland model for $\text{SrCu}_2(\text{BO}_3)_2$, *Phys. Rev. Lett.* **84**, 4461 (2000).
- [58] R. Islam, R. Ma, P. M. Preiss, M. Eric Tai, A. Lukin, M. Rispoli, and M. Greiner, Measuring entanglement entropy in a quantum many-body system, *Nature* **528**, 77 (2015).
- [59] M. Li, M.-J. Zhao, S.-M. Fei, and Z.-X. Wang, Experimental detection of quantum entanglement, *Frontiers of Physics* **8**, 357 (2013).